International Journal of Control and Automation
Vol.8, No.8 (2015), pp.363-372
http://dx.doi.org/10.14257/ijca.2015.8.8.34

Kinematics Modeling and Simulating of a New Surgical Robot

Edris Farah and Liu Shaogang

Harbin Engineering University, College of Mechanical &Electrical Engineering, Harbin - CHINA
edrisfarah@yahoo.com

Abstract

This paper introduced design analysis of a new 5DOF surgical robot used for minimally invasive surgery. The kinematics modeling is studied by solving the forward and inverse kinematics of the robot using the Denavit-Hartenberg convention and geometrical method. Robot kinematics simulation is built by creating the 3D CAD model of the robot and patient, then a kinematic motion simulation of a surgery path tracking is done using CATIA kinematics workbench. The forward and inverse kinematics mathematical models are validated through CATIA simulation models. The comparison results confirm that the kinematics mathematical models of the surgical robot are correct.

Keywords: *surgical robot, Robot kinematic, CATIA, Kinematic simulation*

1. Introduction

Minimally invasive surgery (MIS), also known as laparoscopic surgery, has become increasingly an attractive alternative to open surgery. In MIS, the same operations are performed with specialized instruments which are designed to fit into the body through a several tiny holes instead of one large incision. By summarizing the significant incision, MIS has many benefits over conventional open surgery. It can minimize pain and trauma, and decrease the recovery time, reducing the hospital stay and cost for patients.

However compared to open surgery, MIS offers greater challenges to the surgeons. Instead of looking directly at the part of the body being treated, surgeons monitor the procedures via a two dimensional video monitor, and due to the kinematic constraints of the tools at the incision points, the motions of MIS tools are restricted to four degrees of freedom. In spite of lack of perception and dexterity, all surgeries are moving toward MIS to give more benefits to patients at the cost of more stressful environment to surgeons.

In order to overcome the disadvantages of traditional (MIS), several surgical robotic systems have been develop. Robotic Assisted Minimally Invasive Surgery (RAMIS) presents more dexterity and clearness by carrying enough degrees of freedom for the surgical tool. Using robot in surgery application started by Kwoh when he first used industrial robotic PUMA200 to perform high precision neurosurgical biopsies at the Memorial Medical Center, USA [1]. Sacker and Wang [2], from university of California succeeded to develop a robotic arm for holding the MIS camera (AESOP) Automated Endoscopic System for Optimal Positioning to address the problem of controlling the telescope by hand. The control systems allow the surgeon to place the camera, and leave his hands free to do the other surgery operation on the patient body. The Computer Motion Company, which developed AESOP also, has developed ZEUS telerobotic system in 1998. In this system, AESOP also used to hold the camera with additional of two AESOP to hold surgical instruments. These three units attached to the operating table, and controlled by computers within the surgeon's console. The surgeon control the 3-D position of the tip of each robot arm.

The major challenge in RAMIS is the constrained manipulation of the surgical instrument through a pivot point known as the Remote Center of Motion point (RCM).

ISSN: 2005-4297 IJCA

Taylor and colleagues are the first who performed the (RCM) point notation in surgical robot [3]. In (RCM) the settled fulcrum point is created farther away from the mechanism which free wide area for the surgical instruments to access the affected parts in the patient. The RCM notation has been applied in several surgical robotic systems such as DA Vinici.

In surgical robot kinematics, it is better to determine the kinematics with the dependence of RCM point. The entry RCM point mechanically treated as a fixed point over the entry port in the abdominal wall, it has to be mentioned in the mathematical model for the surgical robot kinematics. In general solving the robot kinematics is computationally complex and normally takes long time to solve because the tasks that will be carried out by the robot are in the Cartesian space, while the robot motors works in joint space. Cartesian space contains the orientation matrix and position vector, while the joint space is described as joint angles. Forward kinematics problems are easy to obtain and no much complexity to solve it, but the inverse kinematic problems are more complex.

Several studies have discussed the kinematics problem for different kind of surgical robots. Navarro et al. presented the kinematics analysis of 3UPS-1S parallel surgical robot using Screw theory [4]. Zhang et al. derived the forward and inverse kinematics for a surgical robot with four degrees of freedom based on systematic method [5]. Paisley et al. provided the forward and inverse kinematics solution for a parallel surgical robot with five degrees of freedom (PARAMIS) using geometrical model [6]. Kuo et al. reviewed the general kinematics design requirements for MIS robots and studied the remote center-of-motion (RCM) mechanism types [7]. Jin et al. defined the forward kinematics and the inverse kinematics for a Pedicle Screws Surgical Robot (PSSR) using the D-H notation [8]. Lum et al. derived the forward and inverse kinematics for spherical serial links mechanism used for surgical applications based on D-H parameters [9]. Zoppi et al. presented the forward and inverse kinematics for four-legged parallel surgical robot using the parametric analytical form solution [10].

In this paper, a solution of a forward and inverse kinematics of a new 5DOF surgical robot have been studied and validated. The mathematical model for the forward and inverse kinematics are created. Kinematics motion simulation of the robot end-effector inside the patient's body is done using CATIA simulation. Robot kinematics mathematical model and simulation model are compared and discussed.

The remainder of this paper is organized as follows: Section 2 presents the forward and inverse kinematics mathematical modeling. The building steps of CATIA kinematics simulation are described in Section 3. The simulation results are discussed in Section 4. Finally, a conclusions are given in Section 5.

2. Forward Kinematics Modeling

Consider the 5DOF surgical robot shown in Figure.1 where the dimensions and skeleton model are presented. Joint axes are assigned to refer to the Denavit-Hartenberg representation. The forward kinematics problem is related to the relationship between the different joints of the manipulator robot and (position and orientation) of the end effector [11, 12]. Angles between links are the joint variables in the case of the revolute joints, or the extension of the link in case of prismatic joints. We will use D-H standard Convention (Table.1) and the geometric model in Figure.2 to find the forward kinematics. The homogeneous transformation matrix which expresses the position and orientation of each link is a product of four basic transformations:

$$A_i = Rot_{z,\theta_i} \times Trans_{z,d_i} \times Trans_{x,a_i} \times Rot_{x,\alpha_i} \quad (1)$$

Multiplying out the above equation, we obtain the general form of the homogeneous transformation matrix:

$$A_i = \begin{bmatrix} C_{\theta_i} & -S_{\theta_i} C_{\alpha_i} & S_{\theta_i} S_{\alpha_i} & a_i C_{\theta_i} \\ S_{\theta_i} & C_{\theta_i} C_{\alpha_i} & -C_{\theta_i} S_{\alpha_i} & a_i S_{\theta_i} \\ 0 & S_{\alpha_i} & C_{\alpha_i} & d_i \\ 0 & 0 & 0 & 1 \end{bmatrix}$$

Where: $C_{\theta_i} = \cos\theta_i ; C_{\alpha_i} = \cos\alpha_i ; S_{\theta_i} = \sin\theta_i ; S_{\alpha_i} = \sin\alpha_i$

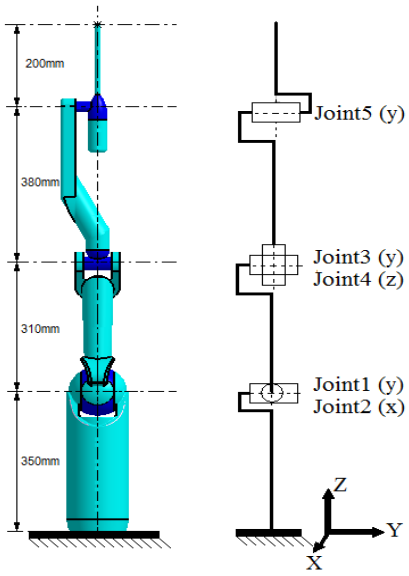

Figure 1. CAD & Skeleton Model of the Surgical Robot

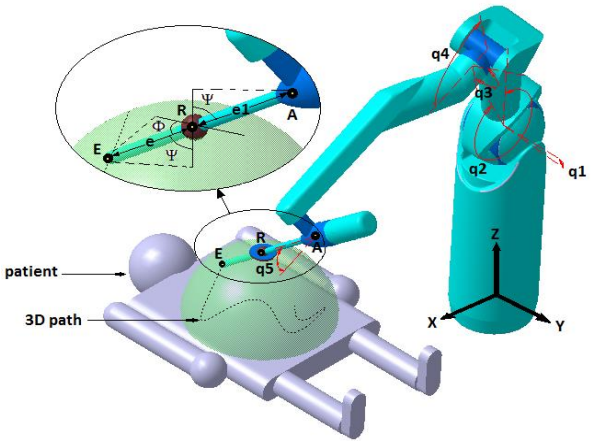

Figure 2. Kinematic Scheme for the Surgical Robot

Table 1. D-H Parameters of the 5DOF Surgical Robot

θ_i	d_i	a_i	α_i
0	350	0	$-\pi/2$
$\theta_1 - \pi/2$	0	0	$\pi/2$

θ_2	0	310	$-\pi/2$
$\theta_3-\pi/2$	0	0	$\pi/2$
θ_4	380	0	$-\pi/2$
θ_5	0	0	$\pi/2$
0	200	0	0

The forward kinematics can be determined by multiplying the transformation matrixes from base to the end-effector, or we can use another solution by considering the constraint of the RCM point (point R in Figure.2) and find the transformation matrixes from base to point A to get the position of point A. Then find the position of point E from point R and point A.

Besides, the two rotation angles $(\phi \text{ and } \psi)$ about x and y axes of the RCM point also have to be found.

Using Maple these matrices are calculated from base to point A:

$$T_0 := \begin{bmatrix} 1 & 0 & 0 & 0 \\ 0 & 0 & 1 & 0 \\ 0 & -1 & 0 & 350 \\ 0 & 0 & 0 & 1 \end{bmatrix} \qquad T_1 := \begin{bmatrix} \sin\theta_1 & 0 & -\cos\theta_1 & 0 \\ -\cos\theta_1 & 0 & -\sin\theta_1 & 0 \\ 0 & 1 & 0 & 0 \\ 0 & 0 & 0 & 1 \end{bmatrix}$$

$$T_2 := \begin{bmatrix} \cos\theta_2 & 0 & -\sin\theta_2 & 310\cos\theta_2 \\ \sin\theta_2 & 0 & \cos\theta_2 & 310\sin\theta_2 \\ 0 & -1 & 0 & 0 \\ 0 & 0 & 0 & 1 \end{bmatrix}$$

$$T_3 := \begin{bmatrix} -\sin\theta_3 & 0 & \cos\theta_3 & 0 \\ \cos\theta_3 & 0 & \sin\theta_3 & 0 \\ 0 & 1 & 0 & 0 \\ 0 & 0 & 0 & 1 \end{bmatrix} \qquad T_4 := \begin{bmatrix} \cos\theta_4 & 0 & -\sin\theta_4 & 0 \\ \sin\theta_4 & 0 & \cos\theta_4 & 0 \\ 0 & -1 & 0 & 380 \\ 0 & 0 & 0 & 1 \end{bmatrix}$$

The position and orientation matrix of A is determined by the product of the above matrices. The last column of the matrix represent the position of point A:

Where:

$$\begin{cases} X_A = 380\sin\theta_1\cos\theta_2\cos\theta_3 + 380\cos\theta_1\sin\theta_3 + 310\sin\theta_1\cos\theta_2 \\ Y_A = 380\sin\theta_2\cos\theta_3 + 310\sin\theta_2 \\ Z_A = 380\cos\theta_1\cos\theta_2\cos\theta_3 - 380\sin\theta_1\sin\theta_3 + 310\cos\theta_1\cos\theta_2 + 350 \end{cases} \tag{2}$$

Angles $(\phi \text{ and } \psi)$ is calculated using point A and point R. From Figure 2, the following equations can be written:

$$\begin{cases} e1 = \sqrt{(X_A - X_R)^2 + (Y_A - Y_R)^2 + (Z_A - Z_R)^2} \\ \phi = \text{asin}\left(\dfrac{\sqrt{(X_A - X_R)^2 + (Y_A - Y_R)^2}}{e1} \right) \\ \psi = \text{asin}\left(\dfrac{Y_R - Y_A}{e1} \right) \end{cases} \quad (3)$$

Once angle $(\phi \text{ and } \psi)$ are determined, the coordinates of the tool tip (point E) can be determined by the following equation system:

$$\begin{cases} X_E = X_A - h \times \sqrt{\sin\phi^2 - \sin\psi^2} \\ Y_E = Y_A + h \times \sin\psi \\ Z_E = Z_A - h \times \cos\phi \end{cases} \quad (4)$$

Where h is tool length (=200mm).

Point E also can be determined by multiplying the transformation matrixes from base to the end tool and get the last column:

$$\begin{cases} X_E = (((-c_2s_1s_3+c_1c_3)c_4-s_1s_2s_4)s_5-200(-c_2c_3s_1-c_1s_3)c_5) \\ \qquad +380(c_2c_3s_1+c_1s_3)+s_1a_3c_2 \\ Y_E = (((-c_1c_2s_3-c_3s_1)c_4-c_1s_2s_4)s_5-200(-c_1c_2c_3+s_1s_3)c_5) \\ \qquad +(c_1c_2c_3-s_1s_3)380+c_1a_3c_2+350 \\ Z_E = 200((-c_4s_2s_3+c_2s_4)s_5+s_2c_3c_5)+380s_2c_3+310s_2 \end{cases} \quad (5)$$

where :
$C_n = \cos\theta_n, S_n = \sin\theta_n$

3. Inverse Kinematics Modeling

For the inverse kinematics model, the position and orientation of the tip of the end-effector (point E) is given; and the joints angles are required. RCM point is considered in the calculation of the inverse kinematics; $(\phi \text{ and } \psi)$ angle are determined using point E (XE, YE, ZE) and point R (XR, YR, ZR) in figure 2. These two angles is used to find the coordinates of point A, once we find point (A); theta_1, 2, and 3 can be determined by solving equation (2). Theta_4 and 5 also can be determined by solving equation (5).

Referring to Figure. 2, once the RCM point is given and point E is given the following equations can be written:

$$\begin{cases} e = \sqrt{(X_R - X_E)^2 + (Y_R - Y_E)^2 + (Z_R - Z_E)^2} \\ \phi = \text{asin}\left(\dfrac{\sqrt{(X_R - X_E)^2 + (Y_R - Y_E)^2}}{e} \right) \\ \psi = \text{asin}\left(\dfrac{Y_E - Y_R}{e} \right) \end{cases} \quad (6)$$

Maple is used to solve equation (2) and find theta_1, 2, and 3, by means of Groebner Basis method [13]. The solution is as follows:

$$\begin{cases} \theta_1 = \arccos\left(\dfrac{M\times(Z_A-350)\times C_2+2\times310\times X_A\times380\times S_3}{2\times310\times(X_A^2+Z_A^2-2\times Z_A\times350+350^2)}\right) \\ \theta_2 = \arcsin\left(\dfrac{2\times310\times Y_A}{M}\right) \\ \theta_3 = \arccos\left(\dfrac{X_A^2+Y_A^2+Z_A^2-2Z_A\times350-310^2+350^2-380^2}{2\times310\times380}\right) \end{cases} \quad (7)$$

Where : $M = X_A^2+Y_A^2+Z_A^2-2Z_A\times350+310^2+350^2-380^2$,

$C_2 = \cos\theta_2, S_3 = \sin\theta_3$

Using Maple the same is done for equation (5) to find theta_4, and 5:

$$\begin{cases} \theta_4 = \arcsin\left(-\dfrac{-Y_E\times C_2+C_1\times S_2(Z_E-350)+X_E\times S_1S_2}{350\times S_5}\right) \\ \theta_5 = \arccos\left(\dfrac{(Z_E-350)C_1C_2C_3+X_EC_1S_3+X_EC_2C_3S_1+W}{200}\right) \end{cases} \quad (8)$$

Where : $W = Y_EC_3S_2 - 310C_3 + (350 - Z_E)S_1S_3 - 380$

4. CATIA Simulation

CATIA5 kinematics simulation for the surgical robot kinematics is created. The following steps were carried out to perform the simulation [14]:

1. The six robot links, the RCM point, and the 3D surgical path are modeled in CATIA5.
2. Assembly model is created including the six links, the RCM, and the patient model as shown in Figure.3.
3. The end tool constraints are created to keep the tool tip on the path.
4. Assembly constraints are converted to five revolute joint and one spherical joint.
5. (Point Curve) joint is created between the tool tip and the path.
6. Six sensors are added to measure the five joint angles and the tool tip position.
7. The (Point Curve) joint is taken as length driven at the desired constant speed 1mm\s.

The output of the simulation is an excel file containing the measured positions of point E and the five joint angles during time, the data in this file is used to validate the forward and inverse kinematics equations.

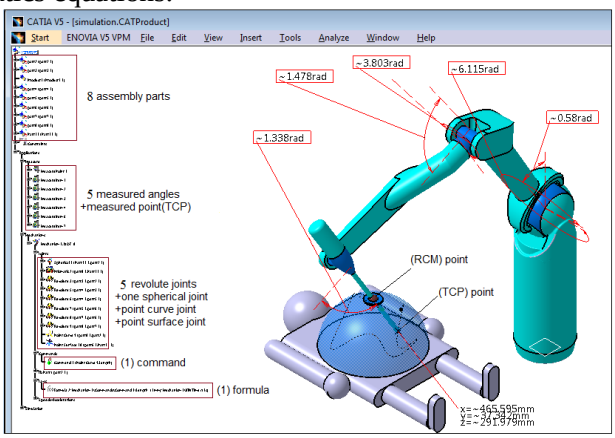

Figure 3. CATIA Model of the Surgical Robot

5. Result and Discussion

CATIA simulation model is created to check the validity of the math model for the forward and inverse kinematics. To get smooth motion, the simulation is implemented by eighty time steps. To check the forward kinematic equations, the five angles data set is taken from the excel file and applied as input to the forward kinematic equations (equation No. 2, 3 and 4). The result is a set of point E (X, Y, and Z) which compared with the measured data of point E in the data file. Figure.4 shows the comparison result between the calculation and simulation result of point E. From the results we one can notice that there is a very small different between the mathematical model and the simulation model. Error in X, Y, and Z direction are shown in Figure 5. Error in X direction varied between (0 to 3mm), in Y direction changed between (-2 to 2mm), and in Z direction varied between (-3 to 0.5mm). So, we can say that all the errors are within the acceptable range.

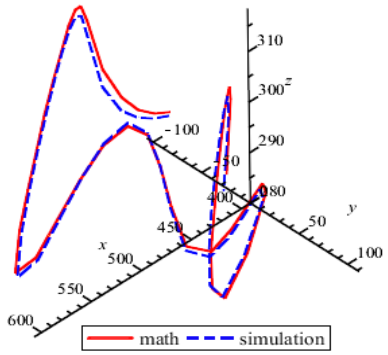

Figure 4. Simulated and Calculated End Tool Motion

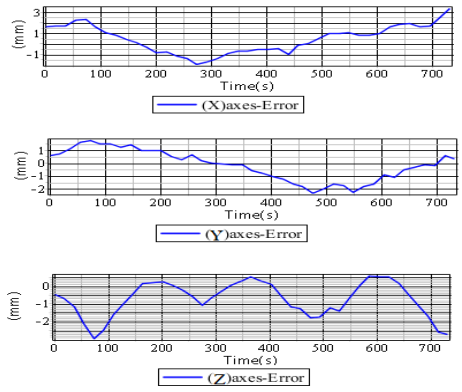

Figure 5. Position Error in X, Y, and Z direction

The second test is done for the inverse kinematics. The RCM point is given as (500, 0,370mm). A set of point E data is taken from the excel file and applied to the angle equations No. 7 and 8. The result angles are compared with the measured angles from the excel file, the validity of each angle is checked. Figure 6 to 10 shows the comparison graphs between the simulation and calculation angles and the error range.

We can notice that there is a very small error for each angle; in Figure 6, theta_1 error varied between (0 to 0.005rad). In Figure 7, theta_2 error varied between (-0.00065 to 0.001rad). In Figure 8, theta_3 error varied between (-0.002 to 0.001rad). In Figure 9, theta_4 error varied between (0 to 0.015rad). In Figure 10, theta_5 error varied between (-

0.007 to -0.002rad). According to the above results, one can say that there is a perfect harmony between the mathematical result and simulation result for all angles, and all errors are within the acceptable range.

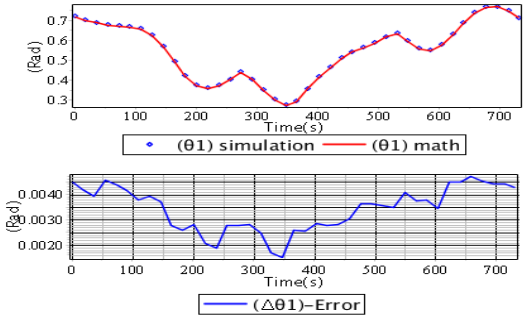

Figure 6. Math and Simulation Model with Error for Theta_1

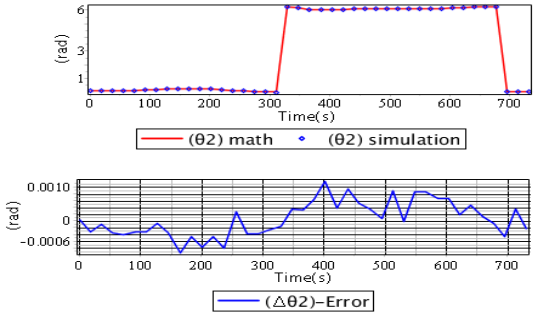

Figure 7. Math and Simulation Model with Error for Theta_2

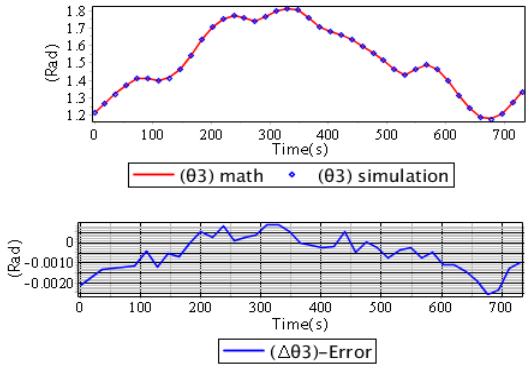

Figure 8. Math and Simulation Model with Error for Theta_3

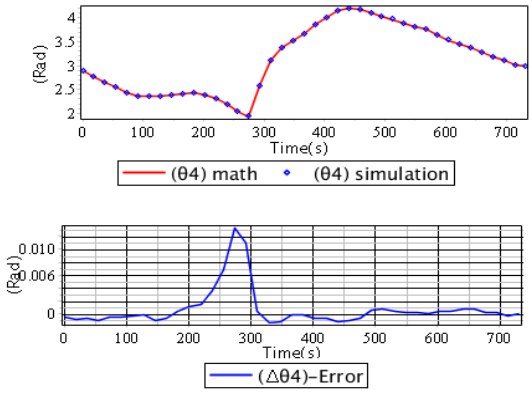

Figure 9. Math and Simulation Model with Error for Theta_4

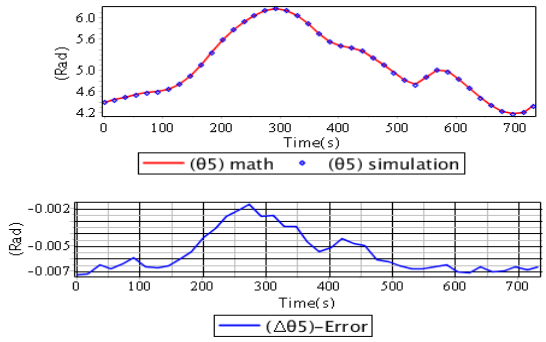

Figure 10. Math and Simulation Model with Error for Theta_5

6. Conclusion

Robot kinematics Modeling and simulating is an important step for robot design and manufacturing. By kinematics Modeling we can estimate and guess the behavior of the robot and optimize the mechanism. The simulation tests smooth the process of designing and allow adjustment before building the real robot.

This paper presented a method to calculate the forward and inverse kinematics of a new 5dof surgical robot using robot geometric model and the Denavit-Hartenberg convention. By using CATIA simulation we have validated the mathematical calculations and examine the validity of the robot to work in surgery environment.

Acknowledgments

The authors gratefully acknowledge the financial support of the International Exchange Program of Harbin Engineering University for innovation and talents cultivation.

References

[1] Kwoh, Y. S., Hou, J., Jonckheere, E. A., & Hayati, S. A robot with improved absolute positioning accuracy for CT guided stereotactic brain surgery. Biomedical Engineering, IEEE Transactions on, **(1988)**. Vol.35, No.2, pp153-160.

[2] Sackier, J. M., & Wang, Y. Robotically assisted laparoscopic surgery. Surgical endoscopy, **(1994)**, Vol.8, No.1, pp.63-66.

[3] Taylor, Russell H., Janez Funda., Ben Eldridge., Steve Gomory., Kreg Gruben., David LaRose., Mark Talamini., Louis Kavoussi., and James Anderson. A telerobotic assistant for laparoscopic surgery. Engineering in Medicine and Biology Magazine, IEEE 14, **(1995),** No. 3, pp. 279-288.

[4] Navarro, J. S., Garcia, N., Perez, C., Fernandez, E., Saltaren, R., & Almonacid, M. Kinematics of a robotic 3UPS1S spherical wrist designed for laparoscopic applications. The International Journal of Medical Robotics and Computer Assisted Surgery, **(2010)**, Vol.6, No.3, pp. 291-300.
[5] Zhang, X., & Nelson, C. A. Kinematic analysis and optimization of a novel robot for surgical tool manipulation. Journal of Medical Devices, **(2008)**, Vol.2, No.2, pp 021003.
[6] Pisla, D., Plitea, N., & Vaida, C. Kinematic modeling and workspace generation for a new parallel robot used in minimally invasive surgery. In Advances in robot kinematics: analysis and design, Springer Netherlands **(2008)**, pp. 459-468.
[7] Kuo, C. H., Dai, J. S., & Dasgupta, P. Kinematic design considerations for minimally invasive surgical robots: an overview. The International Journal of Medical Robotics and Computer Assisted Surgery, **(2012)**, Vol.8, No.2, pp127-145.
[8] Jin, H., Zhang, P., Hu, Y., Zhang, J., & Zheng, Z. (2010, December). Design and Kinematic Analysis of A Pedicle Screws Surgical Robot. In Robotics and Biomimetics (ROBIO), IEEE International Conference on (**2010)**, pp. 1364-1369.
[9] Lum, M. J., Rosen, J., Sinanan, M. N., & Hannaford, B. Kinematic optimization of a spherical mechanism for a minimally invasive surgical robot. In Robotics and Automation, Proceedings. ICRA'04. IEEE International Conference on (**2004)**, Vol. 1, pp. 829-834.
[10] Zoppi, M., Zlatanov, D., & Gosselin, C. M. Analytical kinematics models and special geometries of a class of 4-DOF parallel mechanisms. Robotics, IEEE Transactions on, **(2005)**, Vol.21, No.6, pp1046-1055.
[11] Craig, J. J. Introduction to robotics: mechanics and control. Upper Saddle River, NJ, USA: Pearson/Prentice Hall, pp. 144-146, **(2005)**.
[12] Spong, M. W., Hutchinson, S., & Vidyasagar, M. Robot modeling and control, Vol. 3. New York: Wiley, **(2006)**.
[13] Heck, A., & Koepf, W. Introduction to MAPLE. New York: Springer-Verlag. **(1993)**.
[14] Zamani, N. G., & Weaver, J. M. CATIA V5 Tutorials: Mechanism Design & Animation; Release 19. SDC Publications, **(2010)**.

Authors

Edris Farah, his nationality is Sudanese. He received his M.S. degree in mechanical engineering from KARARY University Sudan. He is currently a PhD student in Harbin Engineering University China. His research interest is in surgical robotic systems.

Liu Shaogang, he is Professor, doctoral tutor. Harbin Engineering University, mechanical design and theory research on design and theory of mechanical discipline leaders, director of the Institute and the government of Heilongjiang province science and Technology Economic Advisory Committee of experts. Currently engaged in mechanical and electronic engineering, mechanical design and theory, computer control system, pneumatic emission (ejection) research technology, fire protection technology, ecological protection technology and equipment. He has many publication in a scholar journal in the above research areas.

